Magnetism in bcc and fcc manganese

G. Fuster,* N. E. Brener, and J. Callaway
Department of Physics and Astronomy, Louisiana State University, Baton Rouge, Louisiana 70803

J. L. Fry and Y. Z. Zhao
Department of Physics, The University of Texas at Arlington, Arlington, Texas 76019

D. A. Papaconstantopoulos
Naval Research Laboratory, Washington, D.C. 20375
(Received 9 November 1987; revised manuscript received 17 February 1988)

Density-functional theory is used to compute the ferromagnetic moment as a function of lattice constant for bcc and fcc Mn. For bcc Mn, a relatively small moment is found in the lattice-constant range $5.20 < a < 6.025$ a.u. and a large moment is found in the region $a > 5.90$ a.u., with a discontinuous low-spin to high-spin transition occurring somewhere in the double-moment region $5.90 < a < 6.025$ a.u. For fcc Mn, the moment is found to be zero in the range $6.50 < a < \sim 7.275$ a.u. and large in the region $a > \sim 7.275$ a.u., with a discontinuous zero-moment to high-moment transition occurring near $a = 7.275$ a.u. Information obtained from magnetic susceptibility calculations is used to predict the magnetic order of the ground state in some of the lattice-constant ranges considered. The susceptibility calculations indicate that bcc Mn has a ferromagnetic ground state in the range $5.2 < a < 5.4$ a.u. and that fcc Mn has an antiferromagnetic ground state in the region $a > 6.8$ a.u.

I. INTRODUCTION

The body-centered-cubic (bcc) and face-centered-cubic (fcc) phases of Mn exist naturally at temperatures that are too high for any type of magnetic order to occur.[1] The stable room-temperature phase of Mn is complex bcc with 29 atoms per unit cell and is known to be antiferromagnetic at low temperature. The question arises as to what magnetic structure the high-temperature phases of Mn (bcc and fcc) would have if they could be maintained at room temperature or below.

Recent experimental work has shown that metastable or alternate phases of transition metals can be stabilized by epitaxial growth on appropriate substrates. In particular, Prinz[2] has used molecular-beam epitaxy (MBE) to stabilize bcc Co (Co is normally hcp) on a (110) substrate of fcc GaAs at room temperature. By appropriate matching of the substrate to the desired structure and lattice constant of the epitaxial layer, Prinz was able to grow a bcc Co layer that is thick enough to display bulk properties and then measure a ferromagnetic moment of $1.53\mu_B$ in this layer, thereby demonstrating that bcc Co is ferromagnetic at room temperature. Using similar techniques, Arrott[3] has succeeded in growing bcc Mn on a (100) Fe substrate. While Arrott did not detect ferromagnetism in the bcc Mn layer at this particular lattice constant, his work demonstrates that bcc Mn, like bcc Co, can be stabilized at room temperature and below by epitaxial growth, and suggests that layers of bcc Mn could be produced at other lattice constants by appropriate choice of substrates. The question then arises as to how the magnetic structure of bcc Mn depends on lattice constant. The question of particular interest is whether bcc Mn, and also fcc Mn, have a range of lattice constants in which ferromagnetism would be expected to occur at low temperature. In this paper we use spin-polarized band-structure and magnetic susceptibility calculations to describe the magnetic structure of bcc and fcc Mn as a function of lattice constant or volume.

Earlier theoretical work in this area includes that of Kubler[4] who used the augmented-spherical-wave (ASW) method[5] to calculate the total energy and magnetic moment of bcc Mn at a single lattice constant (5.82 a.u.) for the ferromagnetic, antiferromagnetic, and nonmagnetic states. He found an antiferromagnetic state to be preferred energetically to the other two at this lattice constant and also found a large magnetic moment for both the ferromagnetic and antiferromagnetic states.

Detailed studies of the magnetic moment versus lattice constant for bcc and fcc Fe were performed by Andersen and co-workers[6–8] using the canonical band method, by Kubler[9] using the ASW method, and by Bagayoko and Callaway[10] using the linear combination of Gaussian orbitals (LCGO) method[11,12] and the program BANDPACKAGE.[13] Kubler, and Bagayoko and Callaway found similar behavior for the ferromagnetic moment as a function of lattice constant. For bcc Fe they found the moment to be a smoothly increasing function of atomic volume. In contrast, they found that the moment in fcc Fe rises abruptly from a small value to a large value as the lattice constant increases, indicating a transition from a low-spin to a high-spin state. This type of transition was first described theoretically by Madsen and Andersen.[6] Bagayoko and Callaway also showed that the bcc and fcc moment curves approach each other closely as the atomic separation increases and explained the abrupt

rise in the fcc moment in terms of the band structure. Subsequently, Moruzzi *et al.*[14] employed the ASW method and the fixed-moment procedure to study the dependence of the total energy on magnetic moment and lattice constant for bcc and fcc Fe, Co, and Ni. For fcc Fe, they obtained the same general behavior of moment versus lattice constant that had been found by the previous workers, including the low-spin to high-spin transition. In addition, Moruzzi *et al.* examined this transition in detail and showed that it is actually discontinuous with a narrow region of overlap in which both the low-spin and high-spin states coexist. Neither Bagayoko and Callaway nor Moruzzi *et al.* considered the possibility of antiferromagnetism in their calculations.

Recently Fry *et al.*[15] employed the LCGO method and BANDPACKAGE program to calculate the ferromagnetic moment versus lattice constant curve for bcc Mn and found behavior similar to that for fcc Fe, including an abrupt low-spin to high-spin transition. They also computed the wave-vector-dependent enhanced magnetic susceptibility for bcc Mn. Based on the magnetic moment and susceptibility calculations, they predicted the occurrence of ferromagnetism in bcc Mn at low temperature. In this paper we continue the work of Fry *et al.* on bcc Mn by examining the nature of the low-spin to high-spin transition in more detail, describing this transition in terms of the band structure and density of states, and performing more susceptibility calculations. In addition, we extend this work to fcc Mn where a transition from zero moment to high moment is found as the atomic volume increases. Enhanced magnetic susceptibility calculations for both bcc and fcc Mn are used to predict whether the ground state is ferromagnetic or antiferromagnetic in certain ranges of lattice constant.

II. BAND-STRUCTURE AND MAGNETIC-MOMENT CALCULATIONS

We employed the program BANDPACKAGE,[13] which has been used previously by Callaway and co-workers in a number of calculations on transition metals,[10–12,16–18] to perform self-consistent, spin-polarized, all-electron calculations of the band structure and magnetic moment of bcc and fcc Mn. The von Barth–Hedin form of the local-density exchange-correlation potential,[19] as parametrized by Rajagopal *et al.*,[20] was used in these calculations. The convergence criterions used were 10^{-4} Ry for the energies and $10^{-4}\mu_B$ for the magnetic moment. We employed the Wachters basis set[21] for Mn except that the most diffuse s-orbital exponent was deleted and a single f orbital of exponent 0.8 was added. All orbitals in the basis set were treated as individual orbitals (no contractions were used), giving 1 f, 5 d, 10 p, and 13 s orbitals for a total of 75 basis functions. The calculations were done for a number of different lattice constants for both bcc and fcc Mn, as described below.

At larger lattice constants, the Mn basis set described above becomes inadequate and additional diffuse orbitals must be added. Consequently, bcc moment calculations at $a=7.0$, 8.0, and 9.0 a.u., and fcc moment calculations at $a=9.0$ a.u. were done with an expanded basis set containing two additional s-orbital exponents (0.27378 and 0.06541), one additional p exponent (0.07831), and two additional d exponents (0.18212 and 0.08550). For lattice constants smaller than the above values, the additional diffuse orbitals were found to be unnecessary and the moment calculations were done with the basis set given in the preceding paragraph.

Our calculations consider nonmagnetic and ferromagnetic states only as the band program currently in use cannot be employed for the lower-symmetry antiferromagnetic state. It is possible that the ground state of these materials is antiferromagnetic, particularly at large lattice constants. Some information concerning the probable magnetic order of the ground state which can be derived from magnetic susceptibility calculations is discussed in Sec. III.

A. bcc Mn

Table I gives the computed ferromagnetic moment for bcc Mn at a number of different lattice constants in the range 5.2–9.0 a.u. The table shows that the moment undergoes a low-spin to high-spin transition somewhere in a lattice-constant range of 5.90–6.025 a.u. In this narrow range of transition, both the low-spin and high-spin moments coexist, as shown by columns 2 and 3 of the table. The transition from low moment to high moment is discontinuous and occurs at a point in this narrow double-moment region. Since the total energy was not computed, we cannot determine the precise value of lattice constant at which the transition occurs, however, this has little effect on the overall moment versus lattice-constant curve since the transition region is very narrow. This type of discontinuous low-spin to high-spin transition with a narrow double-moment region is similar to that found by Moruzzi *et al.* for fcc Fe.

The results of Table I are shown graphically by the solid line in Fig. 1, which gives the ferromagnetic moment versus lattice constant curve for bcc Mn. As shown by Fig. 1, the moment has a relatively small value in the

TABLE I. Lattice constant a and ferromagnetic moment m for bcc Mn. Indices 1 and 2 refer to the low-spin and high-spin states, respectively.

a (a.u.)	m_1 (units of μ_B)	m_2 (units of μ_B)
5.200	0.76	
5.397	0.93	
5.450	0.97	
5.628	1.09	
5.800	1.18	
5.900	1.24	2.40
5.925	1.26	2.93
5.950	1.28	3.12
5.975	1.29	3.40
6.000	1.32	3.49
6.025	1.35	3.53
6.050		3.56
7.000		4.24
8.000		4.63
9.000		4.93

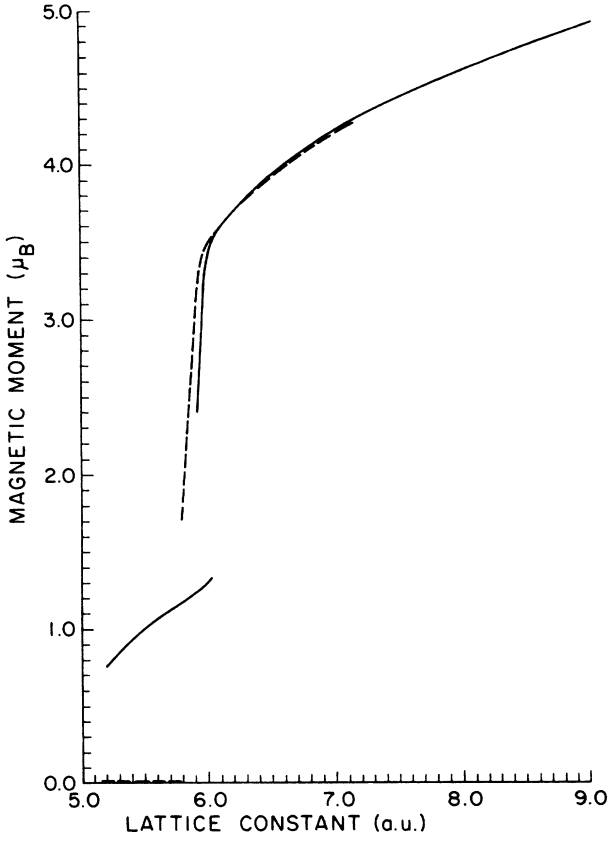

FIG. 1. Ferromagnetic moment of bcc Mn (solid curve) and fcc Mn (dashed curve) vs lattice constant. The fcc curve is plotted versus the bcc equal volume lattice constant which is obtained by dividing the fcc lattice constant by $2^{1/3}$.

lattice-constant range 5.2–6.025 a.u. and a large value in the range 5.90–9.0 a.u., indicating the existence of low-spin and high-spin ferromagnetic states, respectively, in these ranges of volume. The figure indicates that as the lattice constant increases past 9.0 a.u., the moment approaches its maximum possible value of $5\mu_B$, which is the value of the moment of an isolated Mn atom.

The low-spin–high-spin transition in bcc Mn can be related to the band structure and density of states (DOS). As mentioned above, we cannot determine precisely the lattice constant at which this transition occurs, however, any low-spin state and adjacent high-spin state in the double-moment region will illustrate the main features of the band structure and DOS immediately before and after the transition. Accordingly, we will pick the value 5.925 to illustrate the low-moment state immediately before the transition and the point 5.95 to illustrate the high-moment state immediately after the transition. In addition, we will use the lattice constant 6.0 to show how the high-spin moment continues to increase after the transition occurs.

Figures 2 and 3 show the majority- and minority-spin band structure, respectively, for the low-spin state at 5.925 a.u. and the high-spin states at 5.95 and 6.0 a.u., and the left column of Fig. 4 shows the densities of states for these three states. The figures show the region of the band structure near the Fermi level, which is the part relevant to the low-spin–high-spin transition. We see that at 5.925, there is a sharp peak in the majority-spin (spin-up) DOS just above the Fermi level which corresponds to the flat portions of the spin-up band structure that extend from N to P and from N toward Γ. We also note a sharp edge in the minority-spin (spin-down) DOS

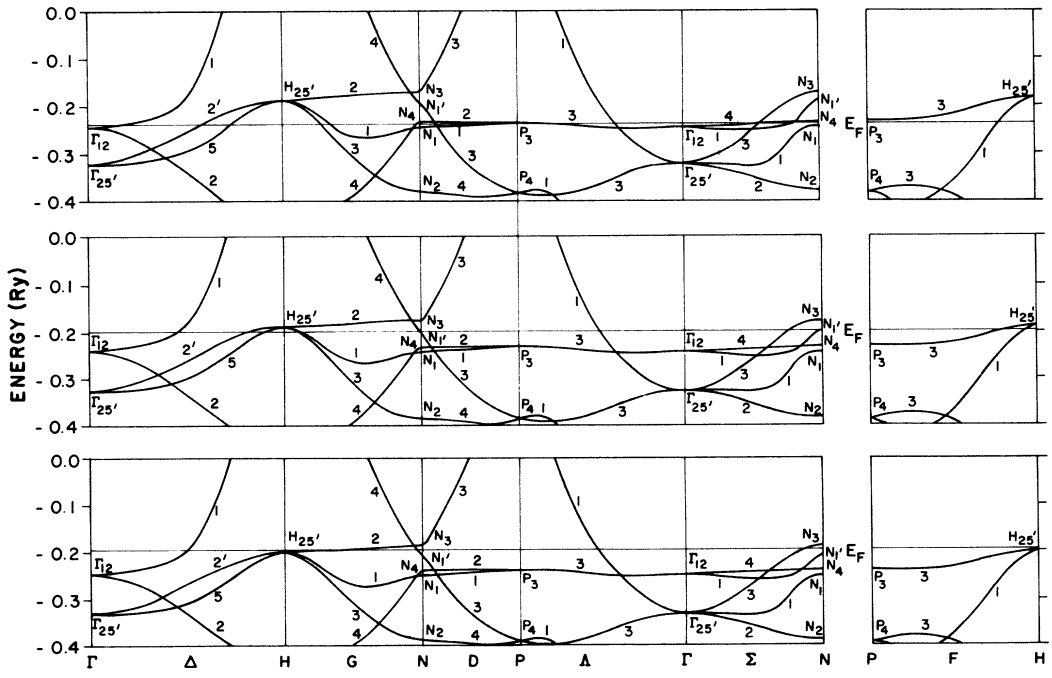

FIG. 2. Majority-spin (spin-up) band structure of bcc Mn at lattice constants of 5.925 a.u. (top), 5.95 a.u. (middle), and 6.0 a.u. (bottom).

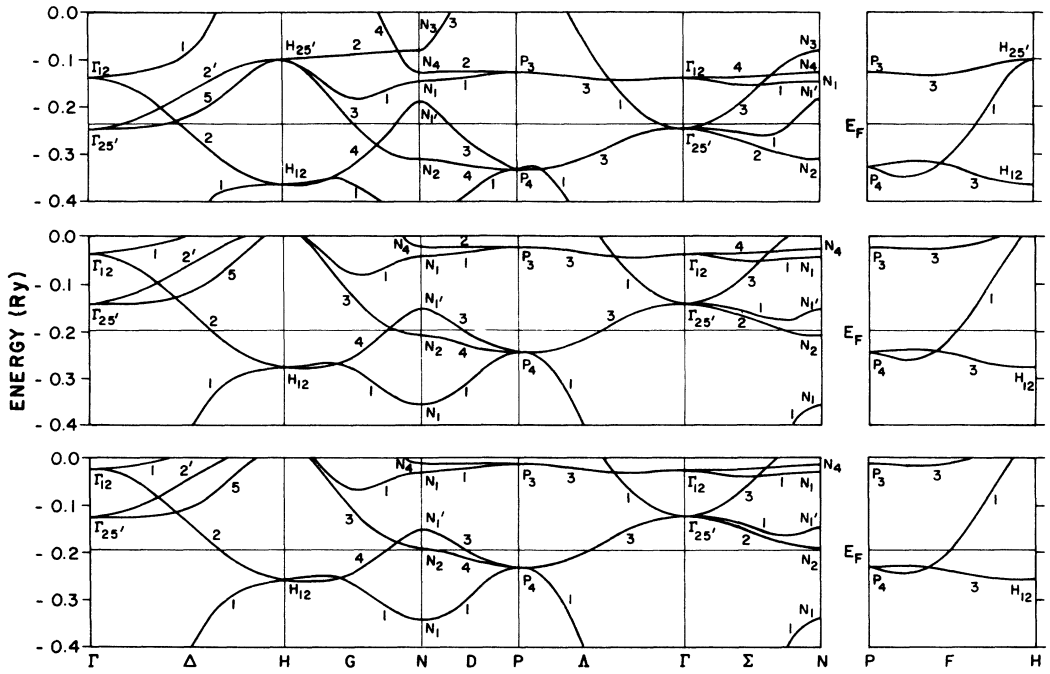

FIG. 3. Minority-spin (spin-down) band structure of bcc Mn at lattice constants of 5.925 a.u. (top), 5.95 a.u. (middle), and 6.0 a.u. (bottom).

that lies a short distance below the Fermi level and corresponds to the flat portions of the spin-down band structure around Γ. Thus a large increase in the moment will suddenly occur when the spin-up peak and spin-down edge simultaneously cross the Fermi level, causing the simultaneous filling of spin-up states and emptying of spin-down states. The DOS and band structure for the high-spin state at 5.95 illustrate the situation just after the transition has occurred, with the spin-up peak now being below the Fermi level and the spin-down edge now being above. At this lattice constant we note further structures in the spin-up DOS that are now just above the Fermi level and which correspond to the flat portions of the band structure around H, and additional structures in the spin-down DOS that are just below the Fermi level and correspond to the flat portions of the spin-down band structure in the vicinity of N. A rapid but continuous increase in the high-spin moment will occur as these additional DOS structures cross the Fermi level, causing simultaneous filling of spin-up states and emptying of spin-down states. The DOS and band structure at 6.0 show the situation after some of these additional spin-up and spin-down structures have crossed the Fermi level. In a similar manner, the high-spin moment will continue to increase, at a slower rate, as further spin-up and spin-down structures continue to simultaneously cross the Fermi level.

Figures 5 and 6 show the band structure of bcc Mn at the lattice constant $a=8.0$ a.u. This band structure was computed with the basis set given in the first paragraph of Sec. II but does not differ significantly from that obtained with the expanded basis set described above. At this expanded volume, the d bands have become very flat, with the majority-spin d states being almost completely occupied and the minority-spin d states being almost completely empty. The only bands that cross the Fermi level are essentially s bands with a very small amount of d hybridization, and consequently the moment is very close to its maximum possible value of $5\mu_B$.

B. fcc Mn

Table II gives the ferromagnetic moment of fcc Mn at a number of lattice constants in the range 6.5–9.0 a.u. The table shows that there is a sudden, discontinuous transition from zero moment to large moment near the lattice constant $a=7.275$ a.u. In this case we do not find a small multiple-moment region at the transition as was found for bcc Mn, but rather find that the transition appears to occur at a single point. It should be noted that this apparent second-order transition in fcc Mn is not of the same type as that reported by Moruzzi[22] for fcc Co. Moruzzi showed that fcc Co has a first-order transition with a small overlap region in which both the nonmagnetic and ferromagnetic states coexist. Further studies are in progress to determine if there is a multiple-moment region that has not yet been resolved by our present calculations. Even if one is found, it would be so narrow that it would have a negligible effect on the overall behavior of the moment versus lattice constant curve. In order to facilitate comparisons with bcc Mn, Table II also gives the equal-volume bcc lattice constant which is obtained by dividing the fcc lattice constant by $2^{1/3}$.

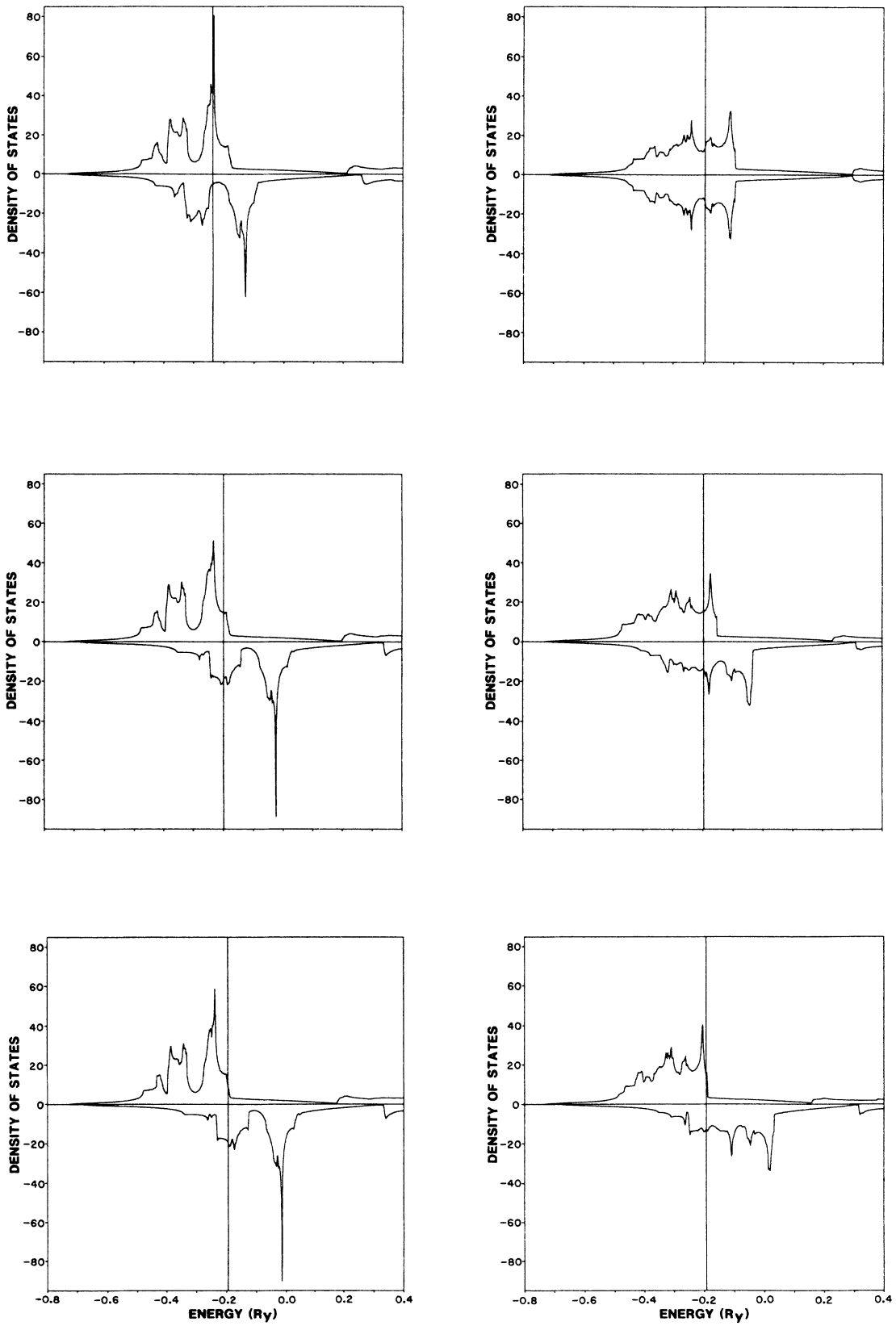

FIG. 4. Density of states (DOS) of bcc Mn at lattice constants of 5.925 a.u. (top left), 5.95 a.u. (middle left), and 6.0 a.u. (bottom left), and DOS of fcc Mn at lattice constants of 7.25 a.u. (top right), 7.3 a.u. (middle right), and 7.5 a.u. (bottom right). The top (bottom) half of each of the six figures is the majority-spin (minority-spin) DOS. The densities of states are in units of states/(atom Ry).

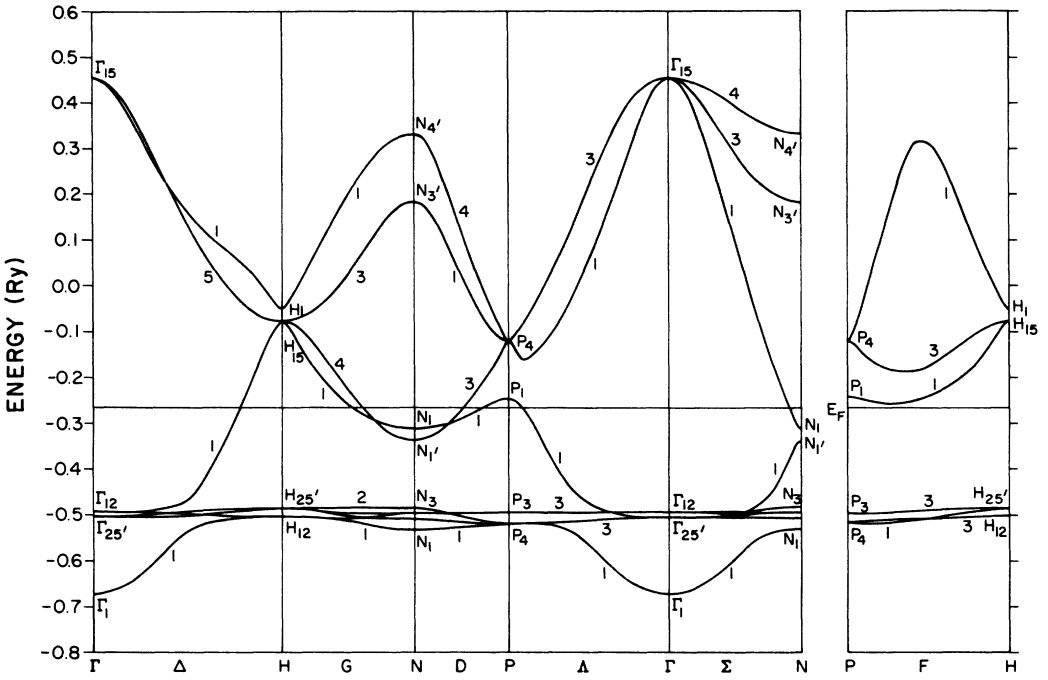

FIG. 5. Majority-spin (spin-up) band structure of bcc Mn at a lattice constant of 8.0 a.u.

The results of Table II are shown graphically by the dashed curve of Fig. 1, which is a plot of the fcc moment versus the bcc equal volume lattice constant. Figure 1 shows that the ferromagnetic moment of fcc Mn is zero for $a_{bcc} < \sim 5.7774$ a.u. ($a < \sim 7.275$ a.u.) and is large for $a_{bcc} > \sim 5.7774$ a.u. ($a > \sim 7.275$ a.u.), indicating the existence of a high-spin ferromagnetic state in this expanded volume region. The figure also shows that as the lattice constant increases, the bcc and fcc high-moment curves approach each other closely, indicating that the moment in the high-spin state in this region is primarily a function of atomic volume rather than of the lattice

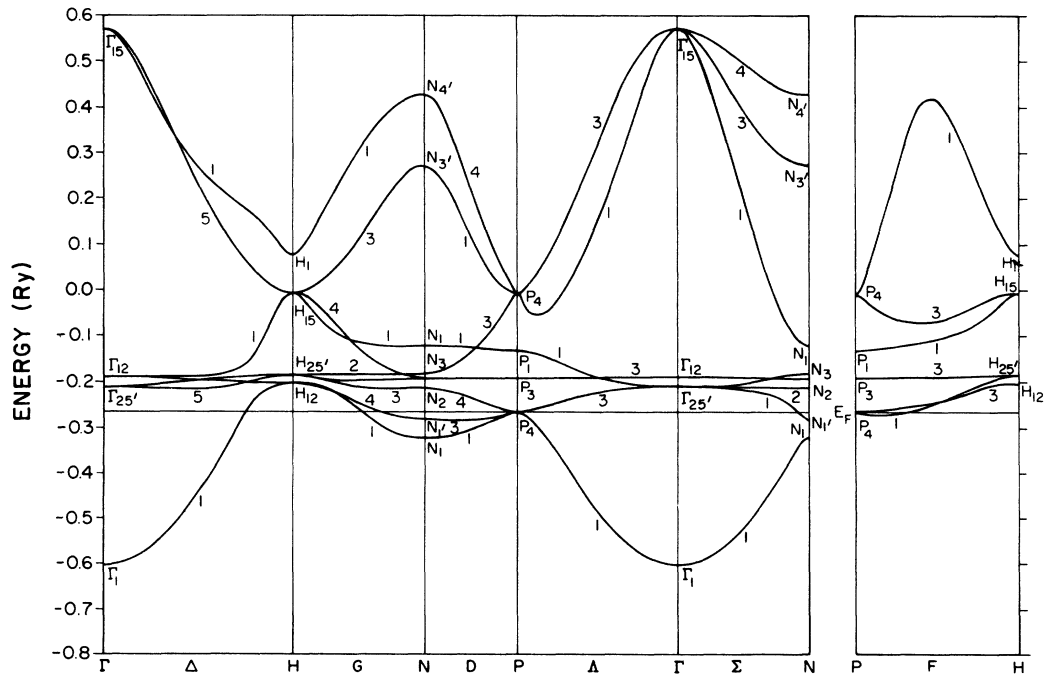

FIG. 6. Minority-spin (spin-down) band structure of bcc Mn at a lattice constant of 8.0 a.u.

TABLE II. Lattice constant a, bcc equal volume lattice constant a_{bcc}, and ferromagnetic moment m for fcc Mn. The bcc equal volume lattice constant is obtained by dividing the fcc lattice constant by $2^{1/3}$.

a (a.u.)	a_{bcc} (a.u.)	m (units of μ_B)
6.50	5.159	0.00
6.75	5.357	0.00
7.000	5.556	0.00
7.200	5.715	0.00
7.250	5.754	0.00
7.275	5.774	1.71
7.300	5.794	1.88
7.400	5.873	2.82
7.450	5.913	3.20
7.500	5.953	3.42
7.600	6.032	3.55
7.700	6.111	3.63
8.000	6.350	3.84
9.000	7.143	4.27

structure. This behavior is similar to that found by Bagayoko and Callaway for bcc and fcc Fe.[10]

As in the case of bcc Mn, the transition to a high moment in fcc Mn can be described in terms of the band structure and DOS. The points $a=7.25$ a.u. and $a=7.3$ a.u. will be used to illustrate the situation immediately before and after the transition, respectively, and the point $a=7.5$ a.u. will be used to show how the moment continues to increase after the transition has occurred. Figures 7 and 8 show the majority- and minority-spin fcc band structure, respectively, for the points $a=7.25$, 7.3, and 7.5 a.u., and the right column of Fig. 4 shows the densities of states at these points. The DOS and band structure at $a=7.25$ a.u. indicate a paramagnetic state, corresponding to the zero moment at this point. We see that at $a=7.25$ a.u., just before the transition, there is a relatively sharp edge in the spin-up DOS just above the Fermi level and a sharp peak in the spin-down DOS that lies a short distance below the Fermi level. The spin-up edge corresponds to the relatively flat unoccupied portions of the band structure around Γ and L, and the spin-down peak corresponds to the flat occupied bands in the vicinity of Γ and L. When this spin-up edge and spin-down peak simultaneously cross the Fermi level, causing simultaneous filling of spin-up states and depletion of spin-down states, the moment will rise discontinuously from zero to a large value. The situation immediately after the transition is illustrated by the band structure and DOS at the point $a=7.3$ a.u., where the spin-up edge (and adjacent structure) and spin-down peak are now below and above the Fermi level, respectively. Additional spin-up and spin-down DOS structures at $a=7.3$ a.u., corresponding to flat unoccupied spin-up bands in the neighborhood of L and to relatively flat occupied spin-down bands around Γ, will cause a rapid but continuous increase in the high spin moment as these additional structures simultaneously cross the Fermi level. The bands and DOS at $a=7.5$ a.u. show the situation after these additional Fermi level crossings have occurred. As in the bcc case, the fcc high-spin moment will continue to increase, at a slower rate, as further majority- and

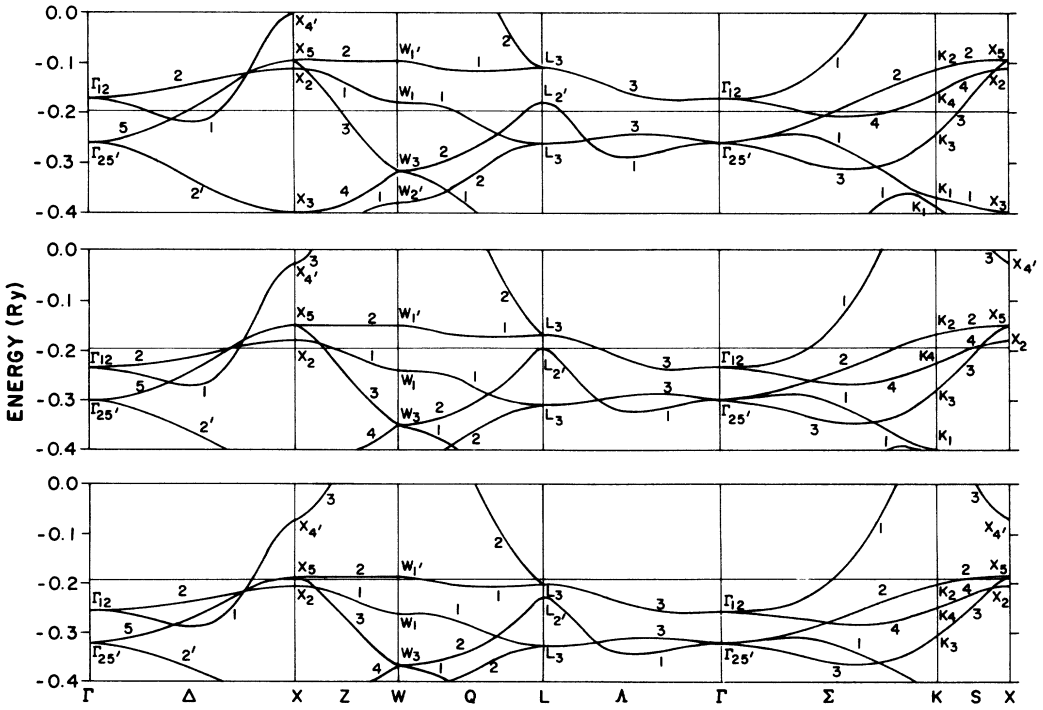

FIG. 7. Majority-spin (spin-up) band structure of fcc Mn at lattice constants of 7.25 a.u. (top), 7.3 a.u. (middle), and 7.5 a.u. (bottom).

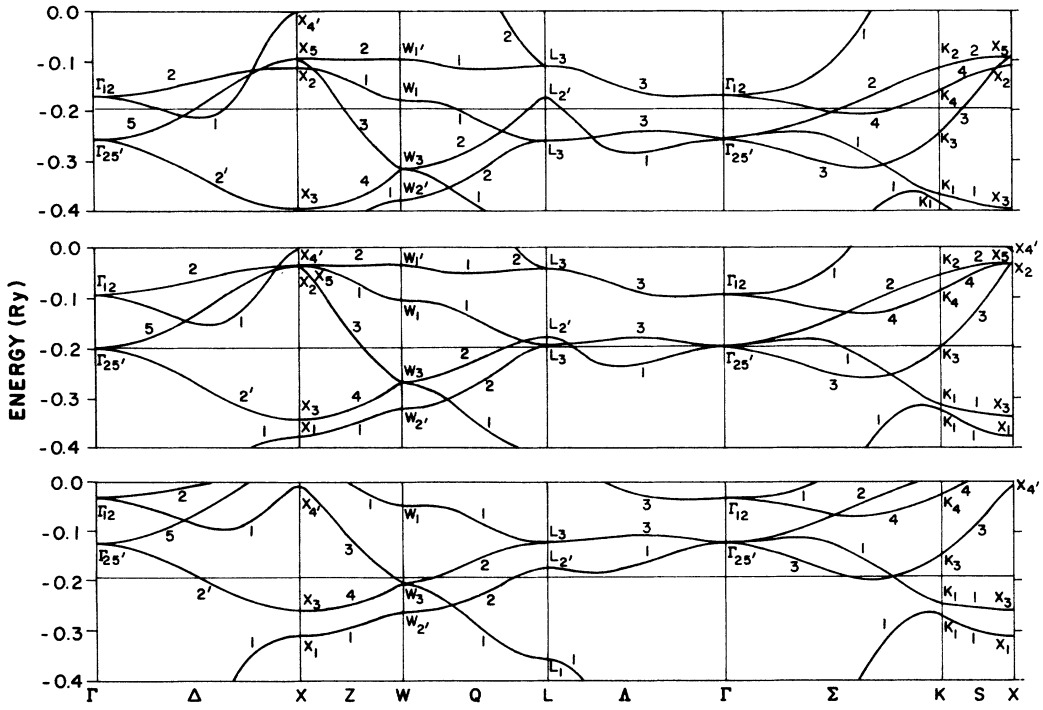

FIG. 8. Minority-spin (spin-down) band structure of fcc Mn at lattice constants of 7.25 a.u. (top), 7.3 a.u. (middle), and 7.5 a.u. (bottom).

minority-spin structures continue to simultaneously cross the Fermi level.

III. MAGNETIC SUSCEPTIBILITY CALCULATIONS AND PREDICTIONS OF MAGNETIC ORDER

The local-density, local-orbital method of Callaway *et al.*[23,24] has been used to compute the wave-vector-dependent enhanced paramagnetic susceptibility for bcc and fcc Mn. The susceptibility calculation is described in more detail in Ref. 15. The Slater-Koster bands of Papaconstantopoulos[25] for paramagnetic bcc Mn at $a=5.397$ a.u. and paramagnetic fcc Mn at $a=6.80$ a.u. were used in the susceptibility calculations. In addition we performed total-energy augmented-plane-wave (APW) calculations on paramagnetic bcc Mn and found a paramagnetic equilibrium lattice constant of 5.20 a.u. The APW band structure at this point was fit by the Slater-Koster method to a tight-binding Hamiltonian in a manner similar to that described in Ref. 25, and the bands so obtained were also used in the susceptibility calculations. Figures 9 and 10 show the wave-vector-dependent susceptibility for bcc Mn at the lattice constants 5.20 and 5.397 a.u., respectively. These figures show both the enhanced susceptibility χ, and the unenhanced susceptibility χ_0 which is a monotonically decreasing function of q within the accuracy of the susceptibility calculation. The enhanced susceptibility curve in both figures resembles that which would be obtained from a Stoner-type formula[26]

$$\chi(q)=\frac{\chi_0(q)}{1-I\chi_0(q)} \tag{1}$$

when $I\chi_0(0)>1$, where I is an enhancement parameter. This behavior of χ and that of χ_0 suggest a ferromagnetic ground state.

In general, the existence of a region of q space in which

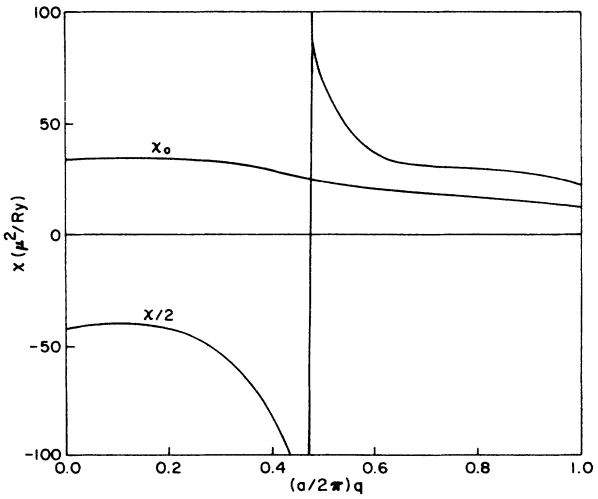

FIG. 9. Unenhanced susceptibility χ_0 and enhanced susceptibility χ for bcc Mn at a lattice constant of 5.2 a.u. χ_0 and χ are plotted along the Δ axis. χ has been divided by 2 to reveal the structure of χ_0.

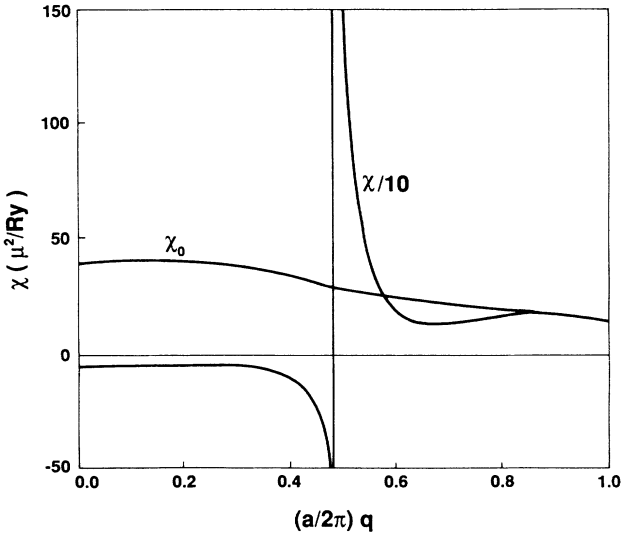

FIG. 10. Unenhanced susceptibility χ_0 and enhanced susceptibility χ for bcc Mn at a lattice constant of 5.397 a.u. χ and χ_0 are plotted along the Δ axis. χ has been divided by 10.

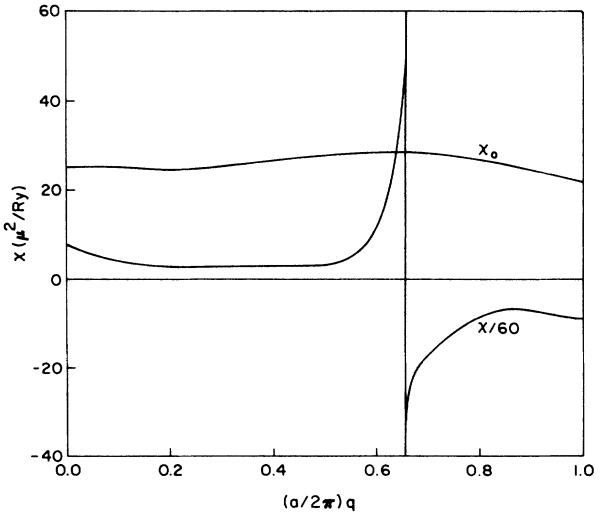

FIG. 11. Unenhanced susceptibility χ_0 and enhanced susceptibility χ for fcc Mn at a lattice constant of 6.8 a.u. χ and χ_0 are plotted along the Δ axis. χ has been divided by 60.

the paramagnetic enhanced susceptibility χ is negative indicates that the paramagnetic (nonmagnetic) state is unstable toward the formation of a magnetically ordered ground state. The particular type of magnetic order that occurs in this ground state is in turn indicated by the q-dependent behavior of the unenhanced susceptibility χ_0. Specifically, the point q at which χ_0 has a maximum (call it q_0) indicates the order of the ground state as follows: if $q_0=0$, the ground state is ferromagnetic; if $q_0\neq 0$, the ground state is antiferromagnetic. Thus negative values of χ and a monotonically decreasing χ_0 point to a ferromagnetic ground state.

Since it is highly unlikely that the ground state of bcc Mn would change from ferromagnetic to antiferromagnetic and then back to ferromagnetic as the lattice constant increases from 5.2 to 5.4 a.u., we predict that bcc Mn has a ferromagnetic ground state everywhere in the lattice-constant range 5.2–5.4 a.u., in particular at the computed ferromagnetic equilibrium lattice constant[27] of 5.28 a.u. Susceptibility calculations are currently in progress to determine whether the ground state of bcc Mn is ferromagnetic or antiferromagnetic at lattice constants greater than 5.4 a.u.

Figure 11 shows the magnetic susceptibility for fcc Mn at the lattice constant $a=6.80$ a.u. The curve for χ resembles that which would be obtained from Eq. (1) when $I\chi_0(q)<1$ for $q=0$, but $\chi_0(q)$ increases with q sufficiently so that $I\chi_0(q)$ passes through 1. This behavior of χ and that of χ_0 indicate that the ground state is probably antiferromagnetic. To state it another way, the features of this susceptibility that suggest antiferromagnetism are the χ_0 maximum at a nonzero q and the negative values of χ. In particular, this susceptibility suggests the occurrence of incommensurate antiferromagnetism. Since in general a tendency toward antiferromagnetism is expected as the lattice constant increases,[28] the fact that the ground state is already antiferromagnetic at $a=6.8$ a.u. indicates that it will probably remain antiferromagnetic as the lattice constant increases past this point. Thus we conclude that the ground state of fcc Mn is probably antiferromagnetic at all lattice constants greater than 6.8 a.u., including the region $a>\sim 7.275$ a.u. where the high-spin ferromagnetic moment was computed. Additional susceptibility calculations currently in progress are expected to confirm the fact that the ground state of fcc Mn is antiferromagnetic in the lattice-constant range $a>\sim 7.275$ a.u.

V. CONCLUSION

We have computed the ferromagnetic moment as a function of lattice constant for both bcc and fcc Mn. For bcc Mn we found a small moment in the lattice-constant range $5.20<a<6.025$ a.u. and a large moment in the range $a>5.90$ a.u. Our calculations revealed a narrow double-moment region, $5.90<a<6.025$ a.u., in which the low-spin and high-spin states coexist, with a discontinuous low-moment to high-moment transition occurring somewhere in this region. For fcc Mn we found a zero moment for $6.50<a<\sim 7.275$ a.u. and a large moment for $a>\sim 7.275$ a.u., with a discontinuous zero-moment to high-moment transition occurring near $a=7.275$ a.u.

The BANDPACKAGE program can consider both nonmagnetic and ferromagnetic states but at present does not permit consideration of a possible antiferromagnetic state. Thus a computed ferromagnetic moment that is greater than zero indicates that the ground state is not nonmagnetic, but the BANDPACKAGE calculations cannot lead to a prediction as to whether the ground state is ferromagnetic or antiferromagnetic. Similarly, a computed moment of zero indicates that the ground state is not ferromagnetic, but the BANDPACKAGE calculations cannot determine whether the ground state is nonmagnetic or antiferromagnetic. The magnetic susceptibility calcula-

tions provide the additional information needed to determine whether or not the ground state is antiferromagnetic at the various lattice constants considered. Susceptibility calculations for bcc Mn at $a=5.20$ a.u. and $a=5.397$ a.u. point to ferromagnetism at both of these lattice constants and indicate that bcc Mn has a ferromagnetic ground state in the range $5.2<a<5.4$ a.u. Additional susceptibility calculations for bcc Mn, which are currently in progress, will be used to determine whether the ground state is ferromagnetic or antiferromagnetic for $a>5.4$ a.u. Susceptibility calculations for fcc Mn at $a=6.80$ a.u. indicate an antiferromagnetic ground state at this point. Consideration of a general tendency toward antiferromagnetism with increasing atomic volume leads to the conclusion that fcc Mn is probably antiferromagnetic everywhere in the region $a>6.80$ a.u. Susceptibility calculations are currently in progress in order to check this conclusion.

ACKNOWLEDGMENT

Research at Louisiana State University was supported in part by the National Science Foundation under Grant No. DMR 85-4259. Work at the University of Texas at Arlington was supported by the Robert A. Welch Foundation under Grant No. Y-707. We are indebted to Dr. Paul Marcus (IBM, Yorktown Heights) for useful correspondence regarding the double-moment transition region.

*Permanent address: Universidad Santa Maria, Valparaiso, Chile.

[1]R. J. Weiss and K. J. Tauer, J. Phys. Chem. Solids **4**, 135 (1958).
[2]G. A. Prinz, Phys. Rev. Lett. **54**, 1051 (1985).
[3]B. Heinrich, A. S. Arrott, J. F. Cochran, C. Liu, and K. Myrtle, J. Vac. Sci. Technol. A **4**, 1376 (1986).
[4]J. Kubler, J. Magn. Magn. Mater. **20**, 107 (1980).
[5]A. R. Williams, J. Kubler, and C. D. Gelatt, Jr., Phys. Rev. B **19**, 6094 (1979).
[6]J. Madsen and O. K. Andersen, in *Magnetism and Magnetic Materials—1975, (Philadelphia), 1976,* Proceedings of the 21st Annual Conference on Magnetism and Magnetic Materials, AIP Conf. Proc. No. 29 edited by J. J. Becker, G. H. Lander, and J. J. Rhyne (AIP, New York, 1976), p. 327.
[7]U. K. Poulsen, J. Kollar, and O. K. Andersen, J. Phys. F **6**, L241 (1976).
[8]O. K. Andersen, J. Madsen, U. K. Poulsen, O. Jepsen, and J. Kollar, Physica B + C **86-88B**, 249 (1977).
[9]J. Kubler, Phys. Lett. **81A**, 81 (1981).
[10]D. Bagayoko and J. Callaway, Phys. Rev. B **28**, 5419 (1983).
[11]C. S. Wang and J. Callaway, Phys. Rev. B **15**, 298 (1977).
[12]J. Callaway and C. S. Wang, Phys. Rev B **16**, 2095 (1977).
[13]C. S. Wang and J. Callaway, Comput. Phys. Commun. **14**, 327 (1978).
[14]V. L. Moruzzi, P. M. Marcus, K. Schwarz, and P. Mohn, Phys. Rev. B **34**, 1784 (1986).
[15]J. L. Fry, Y. Z. Zhao, N. E. Brener, G. Fuster, and J. Callaway, Phys. Rev. B **36**, 868 (1987).
[16]D. G Laurent, C. S. Wang, and J. Callaway, Phys. Rev. B **17**, 455 (1978).
[17]D. G. Laurent, J. Callaway, J. L. Fry, and N. E. Brener, Phys. Rev. B **23**, 4977 (1981).
[18]D. Bagayoko, A. Ziegler, and J. Callaway, Phys. Rev. B **27**, 7046 (1983).
[19]U. von Barth and L. Hedin, J. Phys. C **5**, 1629 (1972).
[20]A. K. Rajagopal, S. P. Singhal, and J. Kimball, Adv. Chem. Phys. **41**, 59 (1979).
[21]A. J. H. Wachters, J. Chem. Phys. **52**, 1033 (1970).
[22]V. L. Moruzzi, Phys. Rev. Lett. **57**, 2211 (1986).
[23]J. Callaway and A. K. Chatterjee, J. Phys. F **8**, 2569 (1978).
[24]J. Callaway, A. K. Chatterjee, S. P. Singhal, and A. Ziegler, Phys. Rev. B **28**, 381B (1983).
[25]D. A. Papaconstantopoulos, *Handbook of the Band Structure of Elemental Solids* (Plenum, New York, 1986).
[26]E. C. Stoner, Proc. R. Soc. Lond. Ser. A **169**, 339 (1939).
[27]P. C. Pattnaik (private communication).
[28]C. Herring, in *Direct Exchange Between Well Separated Atoms,* Vol. 2B of *Magnetism,* edited by G. Rado and H. Suhl (Academic, New York. 1966), p. 1.